nature nanotechnology

LETTERS

PUBLISHED ONLINE: 31 OCTOBER 2010 | DOI: 10.1038/NNANO.2010.209

Ultrasensitive detection and characterization of biomolecules using superchiral fields

E. Hendry[1], T. Carpy[2], J. Johnston[2,3], M. Popland[2], R. V. Mikhaylovskiy[1], A. J. Lapthorn[2], S. M. Kelly[4], L. D. Barron[2], N. Gadegaard[3] and M. Kadodwala[2]*

The spectroscopic analysis of large biomolecules is important in applications such as biomedical diagnostics and pathogen detection[1,2], and spectroscopic techniques can detect such molecules at the nanogram level or lower. However, spectroscopic techniques have not been able to probe the structure of large biomolecules with similar levels of sensitivity. Here, we show that superchiral electromagnetic fields[3], generated by the optical excitation of plasmonic planar chiral metamaterials[4,5], are highly sensitive probes of chiral supramolecular structure. The differences in the effective refractive indices of chiral samples exposed to left- and right-handed superchiral fields are found to be up to 10^6 times greater than those observed in optical polarimetry measurements, thus allowing picogram quantities of adsorbed molecules to be characterized. The largest differences are observed for biomolecules that have chiral planar sheets, such as proteins with high β-sheet content, which suggests that this approach could form the basis for assaying technologies capable of detecting amyloid diseases and certain types of viruses.

The building blocks of life comprise chiral molecular units such as amino acids and sugars, so biomacromolecules formed from these units also exhibit chirality on molecular and supramolecular scales. Chirally sensitive (chiroptical) spectroscopic techniques such as circular dichroism (CD), optical rotatory dispersion (ORD) and Raman optical activity (ROA) are therefore particularly incisive probes of the three-dimensional aspects of biomacromolecular structure, and are widely used in biomolecular science[1,2]. Chiroptical methods typically measure small differences (or dissymmetries) in the interaction of left- and right-circularly polarized light (the chiral probe) with a chiral material[2]. However, the inherent weakness of these existing chiroptical phenomena usually restricts their application to samples at the microgram level. Recently, it has been postulated[3] that under certain circumstances superchiral electromagnetic fields could be produced that display greater chiral asymmetry than circularly polarized plane light waves. We have realized that such superchiral electromagnetic fields are generated in the near fields of planar chiral metamaterials (PCMs), which can greatly enhance the sensitivity of a chiroptical measurement, enabling the detection and characterization of just a few picograms of a chiral material.

PCMs were first fabricated and shown to display large chiroptical effects such as optical rotation by Schwanecke[4], Kuwata-Gonokami[5] and colleagues. The PCMs used in the present study (Fig. 1a) are composed of left- or right-handed (LH/RH) gold gammadions of length 400 nm and thickness 100 nm (plus a 5-nm chromium adhesion layer) deposited on a glass substrate and arranged in a square lattice with a periodicity of 800 nm. As a control, all experiments were repeated using a metamaterial composed of achiral crosses with the same thickness and periodicity as the gammadions: these structures showed no dissymmetry in excitation. Earlier works on PCMs discussed their suitability as negative refractive index materials[6,7] and broadband circular polarizers[8]. Others[9] suggested that the optical excitation of the chiral localized surface plasmon resonances (LSPRs) generates chiral electric fields. For such materials the handedness of the electromagnetic field near the nanoparticle is governed by the chirality of the gammadion; reversal of the chirality of the gammadion reverses the chirality of the generated fields. In this Letter, we demonstrate the potential of using chiral local fields in biosensing technologies.

UV-visible CD spectroscopy was used to probe the optical properties of the PCMs in the presence of a liquid layer (water, TRIS buffer and solutions of the chiral molecules materials). CD spectroscopy determines differences in the extinction spectra of the PCMs that have been obtained with left- and right-circularly polarized light. It has the advantage over conventional UV-visible spectrometry of removing the achiral background of scattered light and achiral plasmonic resonances, considerably simplifying the spectra[1]. The CD spectra from LH and RH PCMs in the presence of water are shown in Fig. 1a. As expected, the spectra of the LH and RH gammadions are essentially mirror images of each other, and small differences in wavelengths and intensities of peaks can be attributed to variations in the level of defects between the LH and RH PCMs. Clear resonances in the CD spectra can be observed, which can be attributed to the excitation of LSPRs in the PCM structures.

A quantitative understanding of the optical properties of the PCMs can be accomplished by application of electromagnetic modelling techniques that allow accurate simulation of the fields in the materials. Such modelling of the PCMs is shown in Fig. 2a, which reproduces the main features observed in the experimental CD spectra, with a slight blueshift and narrowing of the resonances (effects we attribute to rounding of edges and inhomogeneity in the experimental samples). One can clearly see the enhanced electric fields (red areas in the left-hand panels of Fig. 2b–d) caused by coupling to LSPRs in the gold nanostructures. Molecules in these regions will undergo a much stronger interaction with the electromagnetic field than those that lie well away from metallic particles. This means that the dielectric environment of the near surface region of the gammadions will strongly influence the resonant LSPR wavelengths (λ). This phenomenon is the basis of the (bio)-sensing capabilities of nanostructured plasmonic materials[10–15]. The wavelength shift ($\Delta\lambda$) of the LSPR modes of nanoparticles

[1]School of Physics, University of Exeter, Stocker Road, Exeter EX4 4QL, UK, [2]School of Chemistry, Joseph Black Building, University of Glasgow, Glasgow G12 8QQ, UK, [3]Division of Biomedical Engineering, School of Engineering, Rankine Building, University of Glasgow, Glasgow G12 8LT, UK, [4]College of Medical, Veterinary and Life Sciences, Institute of Molecular, Cell & Systems Biology, University of Glasgow, Glasgow G12 8QQ, UK.
*e-mail: malcolmk@chem.gla.ac.uk

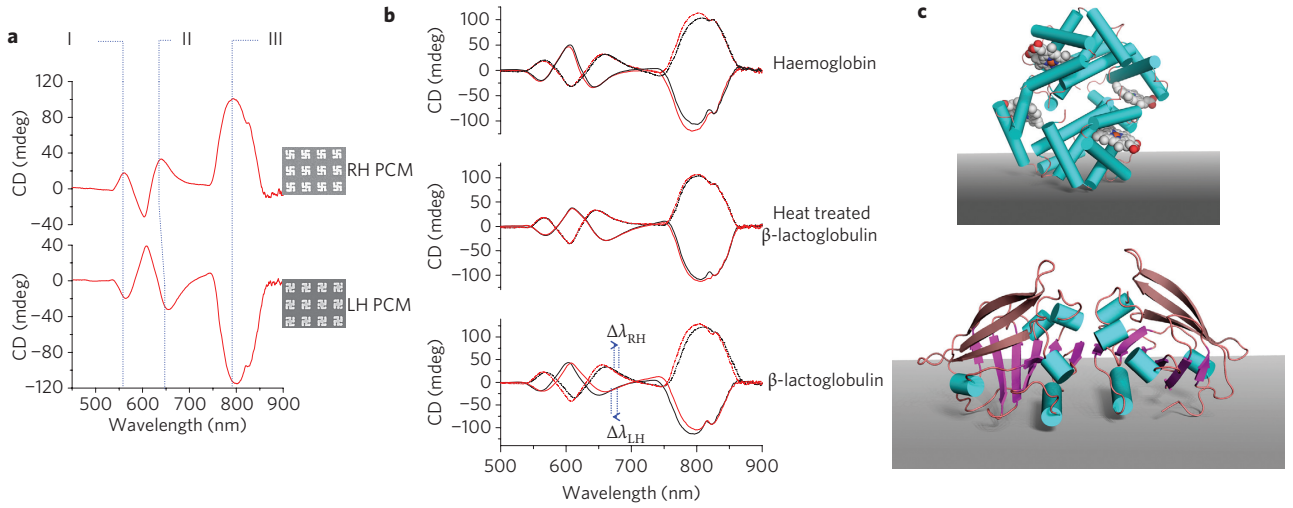

Figure 1 | Changes induced in the chiral plasmonic resonances of the PCM are readily detected using CD spectroscopy. a, CD spectra collected from LH/RH PCMs immersed in distilled water. The three modes that show the largest sensitivity to changes in the local refractive index of the surrounding medium have been labelled I, II and III. Shown to the right of each spectrum is an electron micrograph of the PCM displaying the gammadion structure and periodicity. **b**, Influence of the adsorbed proteins haemoglobin, β-lactoglobulin and thermally denatured β-lactoglobulin on the CD spectra of the PCMs. Red spectra were collected in Tris buffer before protein adsorption (solid line, LH PCM; dashed line, RH PCM), and black spectra were collected after protein adsorption. Magnitudes and directions of $\Delta\lambda_{RH/LH}$ values of mode II for β-lactoglobulin adsorption have been highlighted. **c**, Haemoglobin (upper) and β-lactoglobulin (lower) (α-helix, cyan cylinder; β-sheet, ribbons), shown adopting a well-defined arbitrary structure with respect to a surface. The figure illustrates the more anisotropic nature of adsorbed β-lactoglobulin.

induced by a dielectric layer is normally described approximately by[14,15]

$$\Delta\lambda = m\Delta n\left[1 - \exp\left(-2d/l_d\right)\right] \quad (1)$$

where m is a constant, Δn is the change in effective refractive index (from that of the buffer solution) induced by molecules near the metallic surfaces, d is the thickness of the molecular layer, and l_d represents the spatial evanescent decay of local fields. The quantity m represents the sensitivity of the nanomaterial towards changes in local refractive index, and will be different for each LSPR mode. For the PCMs used in this study, three chiral modes (labelled I, II and III) display the largest m values. These three modes demonstrate the largest $\Delta\lambda$ following changes in the local environment of the gammadions (for example, on changing the refractive index of the surrounding liquid; see Supplementary Information).

As in previous studies[10–15], shifts in the LSPRs are here attributed to adsorption of macromolecules in high field regions, which induces shifts in LSPR wavelengths. We determined how a range of adsorbed chiral materials, with different supramolecular structures, influences the chiral LSPRs. The simplest chiral adsorbate studied here was the amino acid tryptophan, which binds to the surface in a flat geometry by means of its carboxylate group and ring system, forming a planar 'two-dimensional' chiral monolayer[16]. We also studied six proteins: myoglobin, haemoglobin and bovine serum albumin, which have high levels of α-helical secondary structure[18], and β-lactoglobulin, outer membrane protein A (Omp A) and concanavalin A, which have high levels of β-sheet secondary structure[17]. Upon adsorption, protein tertiary structure is strongly modified by the drive to minimize the surface free energy of the interface, but the secondary structure remains largely native[18].

Our data show that the supramolecular structure of an adsorbed chiral layer strongly affects the influence it has on the chiral plasmonic resonances of the PCM. This is demonstrated by the observed shifts in the resonance wavelengths ($\Delta\lambda_{LH}$ and $\Delta\lambda_{RH}$ for LSPRs of the LH and RH PCMs, respectively) induced by adsorption of different molecular species (indicated in Fig. 1b). For the adsorption of some of the chiral molecular layers, the values of $\Delta\lambda_{LH}$ and $\Delta\lambda_{RH}$ are found to be different. We also observe a concurrent asymmetry in the LSPR intensities (note the asymmetry in mode III in the spectra in Fig. 1b). In contrast, for an achiral adsorption layer, no dissymmetry was observed between LH and RH PCMs (we demonstrated this by placing the PCMs in ethanol instead of water; further confirmation was obtained by collecting spectra from PCMs that had films of an achiral molecule deposited upon them, see Supplementary Information). We therefore parameterized the dissymmetries in the shifts of the LSPRs on adsorption of chiral layers using $\Delta\Delta\lambda = \Delta\lambda_{RH} - \Delta\lambda_{LH}$ (see Fig. 3b). The largest values for $\Delta\Delta\lambda$ were found for the adsorption of tryptophan and for the three β-sheet proteins. All three β-sheet protein species induce positive values for $\Delta\Delta\lambda$, whereas tryptophan adsorption gives rise to negative values. The values of $\Delta\Delta\lambda$ have a similar fingerprint for different adsorbed species; modes II and III give rise to the largest dissymmetries, and mode I displays significantly smaller dissymmetries in each case. The large dissymmetries observed for adsorption of tryptophan and the β-sheet proteins do not appear to be associated with the previously reported phenomenon of adsorbate-induced conveying of chirality onto the electronic structures of metals[19–21]; this is demonstrated by the absence of any detected optical activity from achiral crosses after the adsorption of chiral layers (see Supplementary Information). Our observation is also unrelated to the previously reported phenomenon of CD spectra from a biomacromolecule being enhanced in the presence of a plasmonic particle[22,23]. This resonant enhancement arises because an electronic transition of the molecular system overlaps with the plasmonic resonance of the particle. The chiral materials studied have been deliberately chosen so that they do not have an optical excitation that coincides with a resonance of the PCM, to preclude the possibility of observing a plasmonic resonant enhancement.

In contrast to the behaviour found for tryptophan and the three β-sheet proteins, the three α-helical proteins induced comparatively small dissymmetries ($\Delta\Delta\lambda \approx 0$ within experimental error). This behaviour cannot be attributed to lower levels, or even absence, of molecular adsorption. We verified this by monitoring the average shift $\Delta\lambda_{AV} = (\Delta\lambda_{RH} + \Delta\lambda_{LH})/2$ for the PCMs (Fig. 3a), which is a

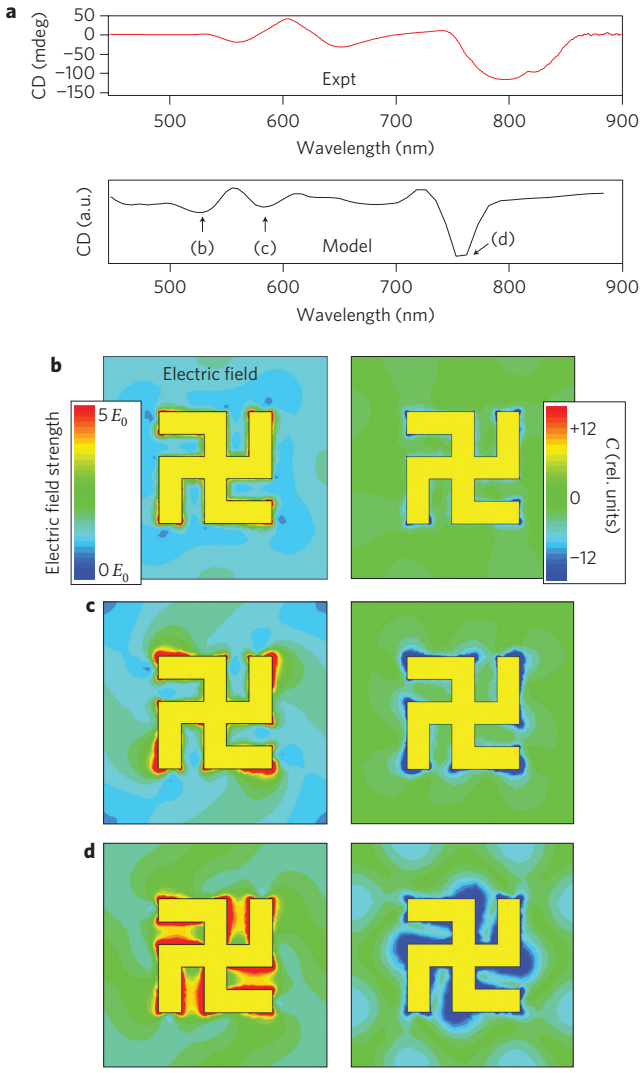

Figure 2 | Finite element modelling of the local electromagnetic fields around the PCMs. a, Comparison between experimental and modelled CD spectra. **b–d**, Left-hand panels: time-averaged electric field strength at the wavelengths marked by arrows in **a**, when excited by LH circularly polarized light. All fields are calculated at the substrate interface of the sample and normalized by the incident electric field (E_0). Right-hand panels: local optical chirality, C, as defined in equation (3), normalized by the magnitudes for LH circularly polarized plane waves.

measure of the thickness of the adsorbed layer. We have further confirmed adsorption levels by implementing surface plasmon resonance (SPR) measurements (see Supplementary Information). Both the SPR and $\Delta\lambda_{AV}$ data demonstrate that there is an appreciable adsorption of α-helical proteins onto the PCM surfaces. We therefore attribute the differences in the dissymmetries exhibited by α-helical and β-sheet proteins to their distinct chiral supramolecular structures. This dependency on macromolecular structure is supported by measurements of β-lactoglobulin layers deposited onto the PCMs from solutions incubated at 70 °C. Previous work has shown that β-lactoglobulin adsorbed from solution at 70 °C onto a metal surface is both aggregated and unfolded, with the loss of β-structure, and exhibits higher levels of adsorption compared to solutions incubated at room temperature[24,25]. We observed a larger $\Delta\lambda_{AV}$ for β-lactoglobulin solutions incubated at 70 °C than for those at room temperature, confirming a higher adsorption of the heat-treated β-lactoglobulin. A markedly smaller observed dissymmetry for heat-treated β-lactoglobulin solutions (Fig. 3b) therefore demonstrates the dependence of dissymmetry on the distinct chiral supramolecular structure associated with the β-sheets.

One can evaluate the strength of the chiral interaction with the adsorbed molecular layers by estimating the dissymmetry in the effective refractive indices of the chiral layers on LH/RH PCMs, $n_{L/R}$. Using the values for $\Delta\Delta\lambda$ from Fig. 3b with equation (1), the following dissymmetry factor g can be determined:

$$g = \frac{n_R - n_L}{(n_R + n_L)} \quad (2)$$

The lower estimates obtained for $|g|$ (see Supplementary Information) for tryptophan and the β-sheet proteins are in the range $\sim 10^{-2} - 10^{-1}$. This magnitude of this dissymmetry is $\sim 10^6$ times that typically observed for the dissymmetries in the refractive indices of the chiral molecules in solution when measured by circularly polarized light ($\sim 10^{-7}$) (refs 1,2).

Local field enhancement (red areas in the left-hand panels of Fig. 2b–d) alone is not sufficient to account for the enhanced chiral response. Owing to the symmetry of the metallic structures in this case, plasmon oscillations in different branches are coupled together to generate superchiral fields. To parameterize the local density of the chirality of an electromagnetic field, others[3] have introduced the following time-even pseudoscalar, termed the optical chirality:

$$C \equiv \frac{\varepsilon_0}{2}\mathbf{E}\cdot\nabla\times\mathbf{E} + \frac{1}{2\mu_0}\mathbf{B}\cdot\nabla\times\mathbf{B} \quad (3)$$

where ε_0 and μ_0 are the permittivity and permeability of free space, respectively, and $\mathbf{E}$ and $\mathbf{B}$ are the local electric and magnetic fields. When considering only dipolar excitation of molecules, the chiral asymmetry in the rate of excitation is given by the product of C with the inherent chiral properties of the material[3]. Tang and Cohen provided an illustration of how superchiral fields might be generated at the nodes of a standing wave, and also suggested that nanostructures may generate fields with locally enhanced chirality. In the right-hand panels of Fig. 2b–d, equation (3) is applied to evaluate the optical chirality of the near fields generated by the present structures: the superchiral field is spatially variable, and is one to two orders of magnitude larger than expected for circularly polarized plane waves. The largest enhancements are clearly observed for modes II and III, whereas mode I exhibits very little enhancement. This observation is consistent with the larger dissymmetries observed for modes II and III in our experiments.

Chiroptical phenomena such as circular dichroism and optical rotation derive from higher-order effects, the largest contributions being from electric dipole–magnetic dipole (dipolar) and electric dipole–electric quadrupole (quadrupolar) interactions, with the latter averaging to zero in isotropic media[2]. Because the definition of optical chirality given in ref. 3 is derived from dipolar excitation molecules, one can expect enhanced optical activity due to the superchiral near fields of the nanoparticles for all the chiral materials studied, including those that form isotropic overlayers on our PCM structures. However, from our electromagnetic modelling we estimate that the enhancement of dipolar chiral excitations due to superchiral fields is at most one to two orders of magnitude, and cannot alone explain the large dissymmetries observed for tryptophan and the β-sheet proteins. We believe that the large dissymmetry enhancements observed for tryptophan and the β-sheet proteins may result from the quadrupolar contribution to optical activity. Under ordinary excitation by circularly polarized light, the dipolar and quadrupolar terms can contribute to the same order of magnitude in anisotropic materials[2]. However, the local chiral field around our PCM structures display steep field gradients,

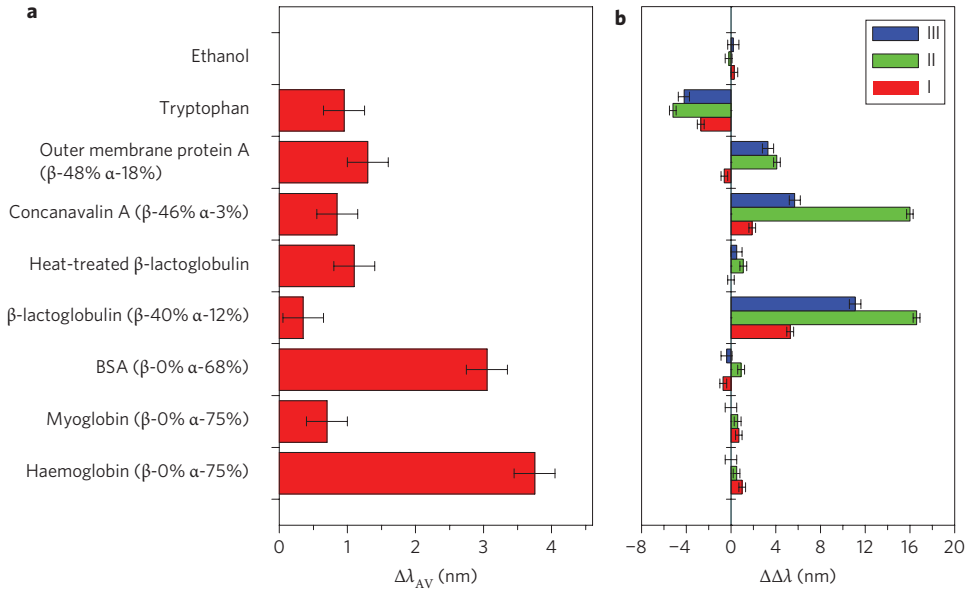

Figure 3 | Values of $\Delta\Delta\lambda$ and $\Delta\lambda_{AV}$ induced by the adsorption of chiral materials. a, Plot of $\Delta\lambda_{AV}$ (I) for tryptophan and the six proteins. **b**, Corresponding $\Delta\Delta\lambda$ values for I, II and III modes. Also shown are the effectively zero $\Delta\Delta\lambda$ values obtained from the (achiral) ethanol solvent.

which will enhance, relative to the dipolar contributions, any quadrupolar contributions to optical activity. Efrima[26] has discussed the influence of the gradients of localized electromagnetic fields on the quadrupolar contribution to the optical activity displayed by an adsorbed anisotropic chiral layer. This work showed that the level of dissymmetry factors such as *g* scale with the gradients of the localized fields. In our electromagnetic modelling (Fig. 2) we observe field gradients near our PCM structures that are three to four orders of magnitude larger than E_0/λ (the value characteristic of plane polarized light). Consequently, quadrupolar contributions to optical activity may give rise to very large dissymmetries for adsorbed anisotropic chiral media.

Upon adsorption, chiral molecules will adopt geometries in which they have an axis with a well-defined orientation with respect to the surface normal, and random orientation in the plane parallel to the surface. Owing to the number and broad spatial distribution of α-helices within myoglobin, haemoglobin and BSA, in the adsorbed state they will be isotropically distributed with respect to the surface (illustrated for haemoglobin in Fig. 1c). For these molecules, one therefore expects the quadrupolar contribution to the dissymmetry to be small. In contrast, the planarity of the adsorbed tryptophan monolayer and β-sheet structures will result in anisotropic adsorbed layers that display C_∞ symmetry (illustrated for β-lactoglobulin in Fig. 1c). The extremely large dissymmetries observed for tryptophan layers and β-sheet proteins therefore reflect the anisotropic structure of the adsorbed layers, which facilitates a large quadrupolar enhancement to the optical activity.

In conclusion, the use of superchiral electromagnetic fields is a new approach to biospectroscopy/biosensing. The phenomenon described here not only allows the detection of the presence of chiral materials at the picogram level, but also determination of their structures. In the future, this will allow, *inter alia*, the monitoring of protein dynamics in ultrasmall (nanofluidic) volumes, and will provide a new ultrasensitive tool for studying chiral macromolecular structure generally. The special sensitivity to β-sheet structure could also provide a unique capability for studying the β-structured amyloid plaques, which play significant roles in diseases such as Alzheimer's, Parkinson's and the transmissible spongiform encephalopathies. The phenomenon might also be used to characterize minute amounts of a virus, and it may be possible to discriminate rapidly between isosahedral viruses (which usually have coat proteins with folds based on β-sheet structure) from cylindrical and filamentous viruses (which usually have α-helical coat proteins folds). Functionalization of the PCMs would, meanwhile, allow a plethora of assay platforms to be developed (for example, protein interactions with other macromolecules, ligands, drugs, the kinetics of fibrillization and so on).

Methods

Experimental set-up. The PCMs were incorporated into a liquid cell with a path length of 90 μm and a total volume of 9 μl. All CD spectra were collected with a side of the PCM lattice parallel to the laboratory frame, and with the back face (metal/glass) of the PCM facing the spectrometer detector (identical spectra were obtained in the reverse geometry when the front face of the PCM faced the detector). A total of $\sim 3.9 \times 10^7$ gammadions were present in the optical path of the spectropolarimeter, and only these contributed to the observed spectra. CD spectra were collected using a commercial spectropolarimeter (JASCO J-810).

Solutions of chiral materials. All solutions were used at a concentration of 1 mg ml^{-1}. The tryptophan solution was made up using distilled water, and the protein solutions were made using a 10 mM Tris/HCl buffer at pH 7.4.

Cleaning procedure. PCM substrates were used in multiple experiments. After each protein adsorption and measurement cycle, the samples were immersed in saline solution for 20 min, followed by 20 min in sodium dodecyl sulphate detergent solution, and rinsed with distilled water after each step. Finally, any remaining (organic) residue was removed in an oxygen plasma-cleaning unit (100 W for 1 min).

Electromagnetic field simulations. Numerical simulations of electromagnetic fields were performed using a commercial finite-element package (Ansoft HFSS version 11.0) with a mesh size of 4.0 nm. Permittivity values for gold were taken from ref. 27. The CD spectrum in Fig. 2a was calculated from the optical rotation of linearly polarized light according to ref. 28. The plots in Fig. 2b–d were calculated for excitation by LH circularly polarized light. Further details of numerical simulations can be found in the Supplementary Information.

Received 7 July 2010; accepted 20 September 2010; published online 31 October 2010

References

1. Fasman, G. D. (ed.) *Circular Dichroism and Conformational Analysis of Biomolecules* (Plenum Press, 1996).
2. Barron, L. D. *Molecular Light Scattering and Optical Activity* 2nd edn (Cambridge Univ. Press, 2004).

3. Tang, Y. & Cohen, A. E. Optical chirality and its interaction with matter. *Phys. Rev. Lett.* **104,** 163901 (2010).
4. Schwanecke, A. S. *et al.* Broken time reversal of light interaction with planar chiral nanostructures. *Phys. Rev. Lett.* **91,** 247404 (2003).
5. Kuwata-Gonokami, M. *et al.* Giant optical activity in quasi-two-dimensional planar nanostructures. *Phys. Rev. Lett.* **95,** 227401 (2005).
6. Pendry, J. B. A chiral route to negative refraction. *Science* **306,** 1353–1355 (2004).
7. Zhang, S., Park, Y. S., Li, J. S., Zhang, W. L. & Zhang, X. Negative refractive index in chiral metamaterials. *Phys. Rev. Lett.* **102,** 023901 (2009).
8. Gansel, J. K. *et al.* Gold helix photonic metamaterial as broadband circular polariser. *Science* **325,** 1513–1515 (2009).
9. Konishi, K., Sugimoto, T., Bai, B., Svirko, Y. & Kuwata-Gonokami, M. Effects of surface plasmon resonances on the optical activity of chiral metal nanogratings. *Opt. Exp.* **15,** 9575–9583 (2007).
10. Willets, K. A. & van Duyne, R. P. Localised surface plasmon resonance spectroscopy and sensing. *Ann. Rev. Phys. Chem.* **58,** 267–297 (2007).
11. Anker, J. N. *et al.* Biosensing with plasmonic nanosensors. *Nature Mater.* **7,** 442–453 (2008).
12. Hall, W. P. *et al.* Calcium-modulated plasmonic switch. *J. Am. Chem. Soc.* **130,** 5836–5837 (2008).
13. Link, S. & El-Sayed, M. A. Spectral properties and relaxation dynamics of surface plasmon electronic oscillations in gold and silver nanodots and nanorods. *J. Phys. Chem. B* **103,** 8410–8426 (1999).
14. Haes, A. J. & van Duyne, R. P. A nanoscale optical biosensor: sensitivity and selectivity of an approach based on the localized surface plasmon resonance spectroscopy of triangular silver nanoparticles. *J. Am. Chem. Soc.* **124,** 10596–10604 (2002).
15. Jung, L. S., Campbell, C. T., Chinowsky, T. M., Mar, M. N. & Yee, S. S. Quantitative interpretation of the response of surface plasmon resonance sensors to adsorbed film. *Langmuir* **14,** 5636–5648 (1998).
16. Zhao, X., Zhao, R. G. & Yang, W. S. Self-assembly of L-tryptophan on the Cu(001) surface. *Langmuir* **18,** 433–438 (2002).
17. Berman, H. M., Henrick, K. & Nakamura, H. Announcing the worldwide protein data bank. *Nat. Struct. Biol.* **10,** 980–980 (2003).
18. Malmsten, M. *Protein Architecture: Interfacing Molecular Assemblies and Immobilization Biotechnology* Ch. 1 (Marcel Dekker, 2000).
19. Mulligan, A. *et al.* Going beyond the physical: instilling chirality onto the electronic structure of a metal. *Angew. Chem. Int. Ed.* **44,** 1830–1833 (2005).
20. Bovet, N., McMillan, N., Gadegaard, N. & Kadodwala, M. Supramolecular assembly facilitating adsorbate-induced chiral electronic states. *J. Phys. Chem. B* **11,** 10005–10011 (2007).
21. Gautier, C. & Burgi, T. Chiral *N*-isobutyryl-cysteine protected gold nanoparticles: preparation, size selection and optical activity in the UV-vis and infrared. *J. Am. Chem. Soc.* **128,** 11079–11087 (2006).
22. Lieberman, I., Shemer, G., Fried, T., Kosower, E. M. & Markovich, G. Plasmon-resonance-enhanced absorption and circular dichroism. *Angew. Chem. Int. Ed.* **47,** 4833–4857 (2008).
23. Baev, A., Samoc, M., Prasad, P. N., Krykunov, M. & Autschbach, J. A quantum chemical approach to the design of chiral negative index materials. *Opt. Express* **15,** 5730–5741 (2007).
24. Arnebrant, T., Barton, K. & Nylander, T. Adsorption of α-lactalbumin and β-lactoglobulin on metal surfaces versus temperature. *J. Coll. Int. Sci.* **119,** 383–390 (1987).
25. Eloffsson, U. M., Paulsson, M. A., Sellers, P. & Arnebrant, T. Adsorption during heat treatment related to the thermal unfolding aggregation of β-lactoglobulin A and B. *J. Coll. Int. Sci.* **183,** 408–415 (1996).
26. Efrima, A. Raman optical activity of molecules adsorbed on metal surfaces: theory. *J. Chem. Phys.* **83,** 1356–1362 (1985).
27. Palik, E. D. *Handbook of Optical Constants of Solids* (Academic, 1985).
28. Cantor, C. R. & Schimmel, P. R. *Biophysical Chemistry* Vol. 2, Ch. 8 (W. H. Freeman, 1980).

Acknowledgements

The authors acknowledge financial support from the Engineering and Physical Sciences Research Council (EPSRC), Biotechnology and Biological Sciences Research Council (BBSRC), Medical Research Council (MRC), Diamond Light Source Ltd and the University of Glasgow. The authors also thank the technical support staff of the James Watt Nanofabrication Centre (University of Glasgow).

Author contributions

M.K. conceived and designed the experiments. T.C., J.J., M.P. and S.K. performed the experiments. R.V.M. and E.H. performed numerical simulations. J.J. and N.G. fabricated the PCMs. E.H., L.D.B. and M.K. analysed the data. A.L. and S.M.K. contributed materials/analysis tools. E.H., A.L., S.M.K., N.G., L.D.B. and M.K. co-wrote the paper.

Additional information

The authors declare no competing financial interests. Supplementary information accompanies this paper at www.nature.com/naturenanotechnology. Reprints and permission information is available online at http://npg.nature.com/reprintsandpermissions/. Correspondence and requests for materials should be addressed to M.K.